

# The heavy-ion time-of-flight spectrometer HiToF\*

Hao-Rui Wang,<sup>1</sup> Cheng-Jian Lin,<sup>1,†</sup> Nan-Ru Ma,<sup>1</sup> Lei Yang,<sup>1,‡</sup> Feng Yang,<sup>1</sup> Hui-Ming Jia,<sup>1</sup> Pei-Wei Wen,<sup>1</sup> Tian-Peng Luo,<sup>1</sup> Chang Chang,<sup>1</sup> Hai-Rui Duan,<sup>1</sup> Song-Xian Zhu,<sup>1</sup> Zhi-Jie Huang,<sup>1</sup> Cheng Yin,<sup>1</sup> Zhi-Jie Huang,<sup>1</sup> Ze-Rui Fan,<sup>1</sup> Ling-Yi Fu,<sup>1</sup> Hui-Yan Li,<sup>1</sup> Shao-Wen Mo,<sup>1</sup> Hao Lu,<sup>1</sup> and Chen-Xu Wu<sup>1</sup>

<sup>1</sup>China Institute for Atomic Energy, 102413 Beijing, China

A heavy-ion time-of-flight spectrometer called HiToF with magnet focusing accomplished by quadrupole triplet lens has been constructed at Beijing Tandem Accelerator National Laboratory, mainly for studies of multi-nucleon transfer reactions at energies near the Coulomb barrier. The spectrometer is equipped a rotating chamber with a diameter of 40 cm and can be rotated in a large angular range from  $-40^\circ$  to  $160^\circ$ . The length from target to the focal plane is 2.7 m, enabling high-precision time-of-flight measurements by two micro-channel-plate detectors with 1.9 m apart and typical time resolution of 120 ps. A multi-sampling position-sensitive ionization chamber for  $\Delta E - E$  measurement is placed on the focal plane, which offers  $\Delta Z/Z$  resolution of  $\frac{1}{50}$ . The setup provides a maximum solid angle  $\Delta\Omega = 20$  msr. An experiment of  $^{32}\text{S} + ^{90,94}\text{Zr}$  at the beam energy of 135 MeV was performed to test the performance. The projectile-like ions were identified clearly with the mass resolution  $\sigma = 0.2$  amu. Results show that the HiToF spectrometer is a powerful setup for studying the mechanism of heavy-ion reactions at low-energies.

Keywords: Time-of-flight spectrometer, Heavy-ion, Multi-nucleon transfer reaction, Quadrupole triplet lens

## I. INTRODUCTION

2 Multi-nucleon transfer (MNT) is considered as a promising method for the production of neutron-rich heavy or super-  
3 heavy nuclei and has been studied in the field of low-energy  
4 nuclear reaction for several decades. Despite significant theoretical and experimental efforts, the mechanism of MNT has  
5 not been so clear yet due to the complex phenomena involving the transfer and/or transport of numerous nucleons [1, 2].

6 Due to the intricacies of the reaction mechanisms involved,  
7 the measurement of MNT products requires improved precision,  
8 placing higher demands on the equipment: i) good mass  
9 (A) and charge (Z) identifications for validation of various re-  
10 action channels; ii) a large acceptance for detection of rare  
11 products that are far from the projectile or target, considering  
12 the steep decrease in cross sections with an increasing num-  
13 ber of transferred nucleons; iii) a good energy resolution for  
14 distinction of a huge number of energy levels populated in a  
15 specific reaction channel.

16 Several detection techniques have been developed for par-  
17 ticle identification, such as the measurement of time-of-flight  
18 (ToF) with a known distance of flight. The relative uncer-  
19 tainty is drastically reduced with a long flight distance. As  
20 a mature method, the E-ToF technique, which measures en-  
21 ergy and ToF simultaneously, has been widely used in stud-  
22 ies on transfer reactions at energies near the Coulomb bar-  
23 rier [3]. The mass resolution, determined by energy and ToF  
24 measurements, reaches  $\sigma = 0.2$  amu. For binary reactions,  
25 the kinematic coincidences technique is an effective method  
26 to enhance energy and mass resolution through methods such

30 as simultaneous measurements of ToF of projectile-like ions  
31 and correlated scattering angles [4].

32 To make further investigation of the mechanism of MNT  
33 reactions, a ToF spectrometer for heavy ion reactions, called  
34 HiToF, was constructed at the HI-13 tandem accelerator of  
35 Beijing Tandem Accelerator National Laboratory. Its de-  
36 sign resembles the spectrometer of PISOLO [5] at Laboratori  
37 Nazionali di Legnaro but with a focusing system including  
38 quadrupole triplet lens. The maximum solid angle covered  
39 by HiToF reaches 20 msr. HiToF is equipped with two micro-  
40 channel-plate detectors dedicated to time-of-flight measure-  
41 ment and a specially designed ionization chamber for energy  
42 measurement and charge identification on the focal plane. A  
43 test experiment has been recently conducted successfully, lay-  
44 ing a solid foundation for the further investigation of multi-  
45 nucleon transfer reactions.

46 The paper is organized as follows. Section II describes  
47 the detection systems and ion optical elements; Section III  
48 presents the recent results of the  $^{32}\text{S} + ^{90,94}\text{Zr}$  test experiment;  
49 Section IV summarizes the results and our conclusions.

## II. SPECTROMETER

51 The HiToF spectrometer mainly consists of an adjustable  
52 detection system and an ion-optical system. It is connected  
53 to a steel-tape sealed rotating chamber with a diameter of 40  
54 cm. The spectrometer can rotate with the chamber as a center,  
55 covering an angular range from  $-40^\circ$  to  $160^\circ$ . A schematic  
56 view of the spectrometer is presented in Fig. 1.

### A. The detection system

57 The detection system includes a ToF measurement that  
58 mainly uses two micro-channel plates (MCP1 and MCP2)  
59 and an energy measurement using a multi-sampling position-  
60 sensitive ionization chamber (IC) installed at the focal plane.

\* This work is supported by the National Key R&D Program of China (Contract No. 2022YFA1602302), the National Natural Science Foundation of China (Grant Nos. U2167204, 12175314 and 12235020) and the Continuous-Support Basic Scientific Research Project.

† Corresponding author, [cjlin@ciae.ac.cn](mailto:cjlin@ciae.ac.cn)

‡ Corresponding author, [yanglei@ciae.ac.cn](mailto:yanglei@ciae.ac.cn)

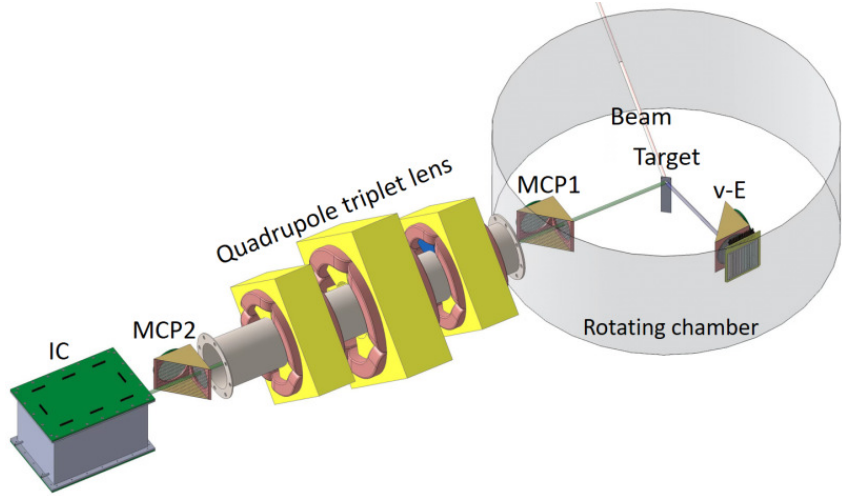


Fig. 1. (Color online) Schematic view of the HiToF spectrometer.

62 A  $v$ - $E$  detector including an MCP and a double-sided silicon-  
 63 strip detector (DSSD) is also installed at the complementary  
 64 angle in the rotating chamber for the velocity and energy mea-  
 65 surements of target-like particles.

66 The ToF measurement consists of two transmission-type  
 67 detectors which have good timing properties, such as timing  
 68 detectors made of micro-channel plates [6]. Two timing de-  
 69 tectors, each using a pair of micro-channel plates with a di-  
 70 ameter of 45 mm, are installed to provide start and stop sig-  
 71 nal along a flight path with a typical timing resolution 120 ps.  
 72 The stop detector is placed at 40 cm from the focal plane. In  
 73 test experiment described in Section III, the start detector was  
 74 set at 40 cm from the target. However, the start detector can  
 75 be placed closer to targets to reduce relative inaccuracy with  
 76 a longer flight distance. Note that both MCP detectors, which  
 77 define the geometrical solid angle for the entire spectrometer,  
 78 can be replaced with a position-sensitive MCP to provide po-  
 79 sition information so that the track of the projectile-like ions  
 80 after magnetic focusing can be reconstructed. The energy  
 81 resolution can be further improved by the ToF information of  
 82 a specific particle. Fig. 2 shows the result of offline test in a  
 83 short flight distance of 5 mm, using a standard  $\alpha$  source.

84 To improve the energy resolution for experimental de-  
 85 mands, a special IC with a transverse electric field has been  
 86 designed. Conventional ionization chambers and active target  
 87 time projection chambers [7, 8] are for references for special  
 88 design of the ionization chamber. The IC is constructed from  
 89 printed circuit boards with dimensions of 300 mm  $\times$  200 mm  
 90  $\times$  200 mm, locating at the focal plane. The length of 300  
 91 mm provides a broad energy range for Z identification. The  
 92 circular entrance window of the IC, which is 100 mm in di-  
 93 ameter, is positioned 18.3 cm away from the second ToF de-  
 94 tector and is equipped with a 2  $\mu$ m thick mylar foil. A large  
 95 area of entrance window provides a large acceptance for en-  
 96 ergy measurement. The grid consists of gold-plated tungsten  
 97 wires with a radius of 0.08 mm, soldered 1 mm apart. The  
 98 distance from grid to anode is 22 mm, while the spacing be-  
 99 tween grid and cathode is 136 mm. 67 equipotential rectangle

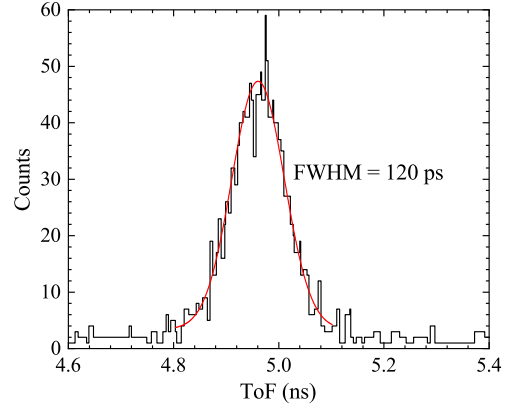


Fig. 2. (Color online) ToF spectrum obtained by a  $\alpha$  source in a short flight distance of 5 mm.

100 shaped loop electrodes are evenly distributed along the plate,  
 101 with resistors of  $1 \text{ M}\Omega$  to connect two adjacent electrodes.

102 This IC is designed with three-dimensional position reso-  
 103 lution capabilities, allowing for precise  $\Delta E - E$  and position  
 104 detection. The energy resolution can be improved by the track  
 105 reconstruction given by the IC. Fig. 3 shows some details of  
 106 the design.

107 The anode of IC is divided into seven sections, which can  
 108 provide not only the energy loss  $\Delta E$  and residual energy  $E_R$ ,  
 109 but also the trajectory (Z-direction) of the entrance ion. Each  
 110 section is divided into two wedge-shaped parts to determine  
 111 the X-position by the charge division method. The Y-position  
 112 is provided by the drift-time difference between anode and  
 113 cathode. The timing signal of MCP2 is also used for the ref-  
 114 erence of the drift-time measurement. Typical X, Y, and Z  
 115 position resolutions are about 1.0, 0.5 and 2.0 mm, respec-  
 116 tively, primarily depending on the properties of entrance ion,  
 117 the working gas as well as the high voltage supplied. The

118 smart preamplifier (SPA) [9] is used for the signal readout  
 119 of IC. Fig. 4 shows the result of offline test, using a fis-  
 120 sion source  $^{252}\text{Cf}$ . The fission fragments of this source have a  
 121 continuous energy spectrum. The working gas is 99.9% pure  
 122 propane with a pressure of 30 torr. The operating voltage is  
 123 110 V for the anode and -308 V for the cathode.

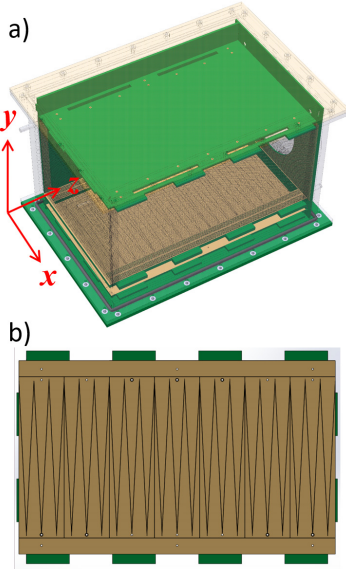


Fig. 3. (Color online) Schematic view of a) IC and b) its anode.

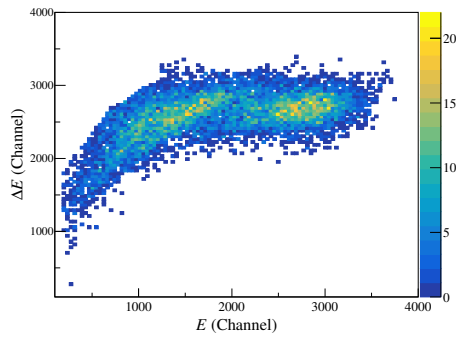


Fig. 4. (Color online)  $\Delta E$  –  $E$  spectrum obtained by a  $^{252}\text{Cf}$  fission source.

124 Practical flight distances are constrained for many techni-  
 125 cal reasons, especially solid angle considerations [10]. Be-  
 126 cause of the optical focusing by the quadrupole triplet lens,  
 127 the real flight distance of the projectile-like particles may de-  
 128 viate from the designated length between start and stop de-  
 129 tectors. For this reason, the X-Y position information at the  
 130 focal plane and the trajectory of the entrance ion provided by  
 131 IC could be used to correct the flight distance, so that the rel-  
 132 ative inaccuracy of the ToF measurement is partly reduced.

## B. The ion-optical system

133 The ion-optical system is designed to use quadrupole triplet  
 134 lens (Q1-Q2-Q3) to transport the entrance ions to the focal  
 135 plane, which is about 2.70 m away from the target. Three  
 136 quadrupole magnets Q1, Q2 and Q3 are equipped at 0.85,  
 137 1.35, 1.85 m from the target. The Q1 and Q3 quadrupoles  
 138 have the same structure with an aperture of  $\Phi_{\text{ape}} = 100$  mm  
 139 and maximum magnetic flux density  $B_{\text{max}} = 0.373$  T. The Q2  
 140 quadrupole locates in the middle, with a reverse-phase cur-  
 141 rent, has an aperture  $\Phi_{\text{ape}} = 130$  mm and a maximum mag-  
 142 netic flux density of  $B_{\text{max}} = 0.636$  T. Ions with a magnetic  
 143 rigidity up to  $B\rho = 0.95$  Tm can be analyzed in the maximum  
 144 angular acceptance  $\Delta\theta = 3.3^\circ$  and  $\Delta\phi = 7.3^\circ$ .

145 The HiToF spectrometer can be operated in three modes:  
 146 a) both X and Y focusing (double-focusing), b) X focus-  
 147 ing and Y parallel, and c) X parallel and Y focusing. The  
 148 double-focusing operation mode, which provides the maxi-  
 149 mum solid angle, enhances the transmission efficiency, and  
 150 mode c) offers a method to preserve the information of the  
 151 scattering angle by focusing only perpendicular to the re-  
 152 action plane [3, 10]. The solid angle of the spectrometer  
 153 was confirmed through the measurement of the yield of all  
 154 quasi-elastic events on the focal plane, as a function of the  
 155 quadrupole field.

156 The corresponding ion trajectories calculated by GICOSY  
 157 code [11] are shown in Fig. 5. The setting of the quadrupole  
 158 triplet lens is mainly determined by the mass, energy and  
 159 charge state of the entrance ion.

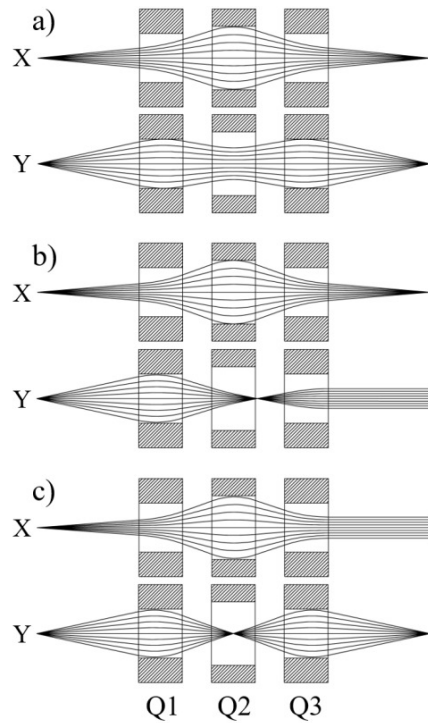


Fig. 5. Ion trajectories of the HiToF spectrometer in three operating modes: a) both X and Y focusing (double focusing), b) X focusing and Y parallel, and c) X parallel and Y focusing.

161

### III. PERFORMANCE OF HITOF

162 An experiment of  $^{32}\text{S} + ^{90,94}\text{Zr}$  at  $E_{\text{Lab}} = 135$  MeV (about  
 163 15% above the Coulomb barrier) has been conducted on the  
 164 spectrometer in order to test its performance. Two targets  
 165 consist of  $^{90}\text{ZrO}_2$  and  $^{94}\text{ZrO}_2$  evaporated onto  $25 \mu\text{g}/\text{cm}^2$   
 166 carbon backings with thicknesses of  $104 \mu\text{g}/\text{cm}^2$  and  $120$   
 167  $\mu\text{g}/\text{cm}^2$  respectively. Focusing performance of magnets, per-  
 168 formance of detection system and the capability of particle  
 169 identification were tested in the experiment.

170 The transmission efficiencies were determined by measur-  
 171 ing the product ions on the focal plane with and without  
 172 magnetic fields. The magnetic fields for maximum transmis-  
 173 sion efficiencies  $B_0$  were set based on GICOSY calculations.  
 174 Several magnetic fields close to  $B_0$  were tested as well. As  
 175 shown in Fig. 6, the enhancement factors of yield ratios with  
 176 and without quadrupole fields for charge states of  $11^+$ ,  $12^+$   
 177 and  $13^+$  in the double-focusing operating mode were in good  
 178 agreement with GICOSY calculations for different magnetic  
 179 fields. In this case, the magnetic field setting for the maxi-  
 180 mum transmission efficiency is  $B_{Q2}/B_{Q1} = 1.678$  with  $B_{Q1} =$   
 181  $B_{Q3}$ .

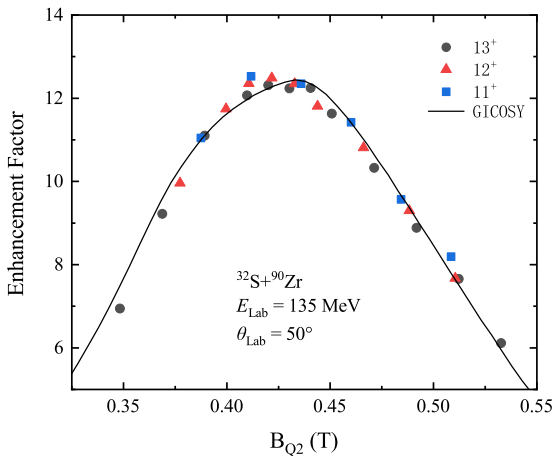


Fig. 6. (Color online) Enhancement factors provided by yield ratios varying with the Q2 field for different charge states. The solid line represents the GICOSY calculation.

182 In the experiment, the ToF was measured between two  
 183 MCP detectors at a flight distance of 1.9 m. The ToF mea-  
 184 surement is influenced by a number of factors such as spec-  
 185 trometer isochronism, target thickness inhomogeneity, energy  
 186 straggling in the target, imperfect software corrections and fi-  
 187 nite resolutions of the ToF detectors [5]. As shown in Fig. 7,  
 188 the FWHM of the main peak of the particle  $^{32}\text{S}$  without mag-  
 189 netic field is 500 ps. The ToF of focused ions is also affected  
 190 by the uncertainty in the flight distance due to the large solid  
 191 angle.

192 Different magnetic fields are required for particles with dif-  
 193 ferent energies, masses and charge states. Additionally, three  
 194 operating modes of focusing were also tested.

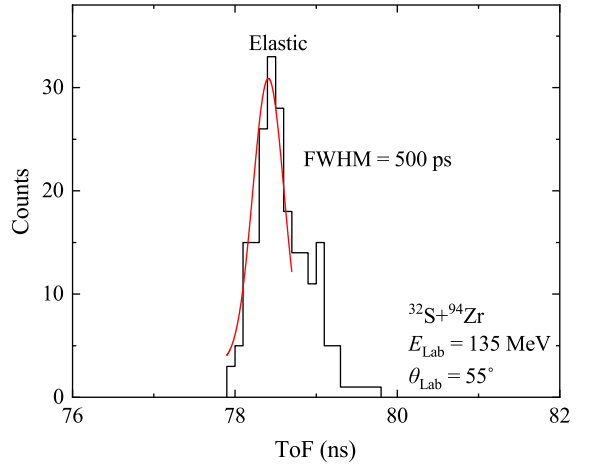


Fig. 7. (Color online) ToF spectrum of  $^{32}\text{S}$  elastic scattering from  $^{94}\text{Zr}$  target.

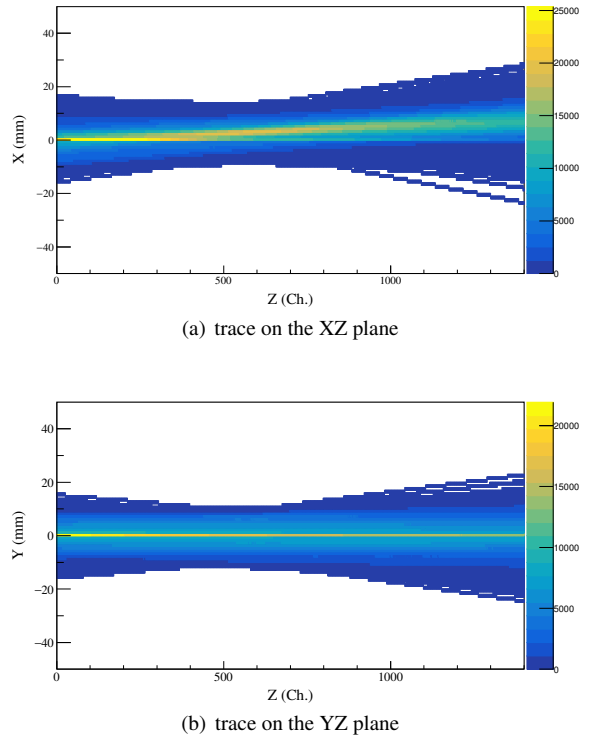


Fig. 8. (Color online) Tracking results of IC in double-focusing mode for the reaction system  $^{32}\text{S} + ^{94}\text{Zr}$  at  $\theta_{\text{Lab}} = 55^\circ$ . (a) trace on the XZ plane (b) trace on the YZ plane.

195 For the test experiment, we redistributed the seven sections  
 196 of the IC anode into three parts of two, two and three sections  
 197 respectively. Propane was used as the working gas for ion-  
 198 ization within a pressure range from 50 to 70 torr. In Fig. 8  
 199 we show the tracking results provided by IC, which is useful

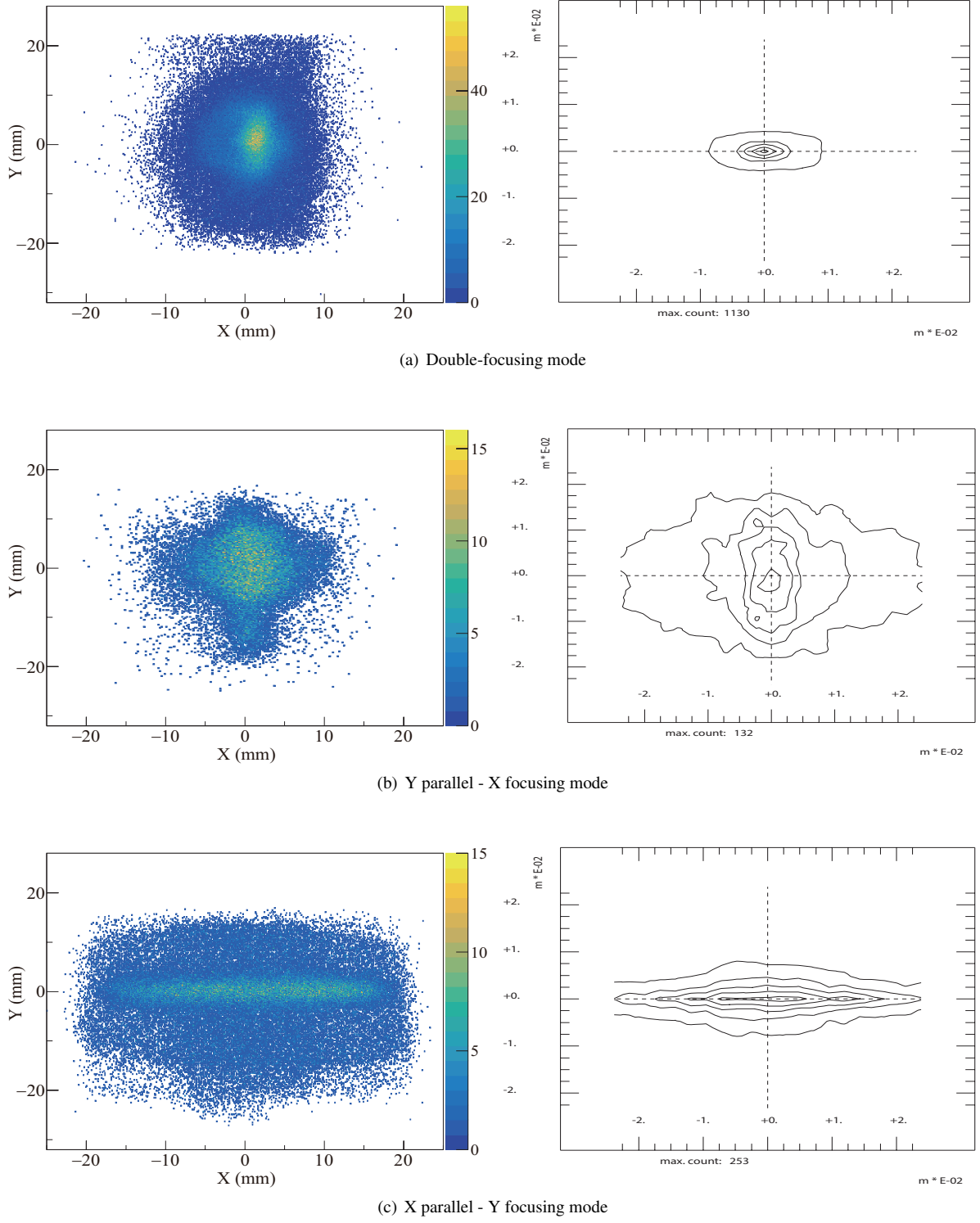


Fig. 9. (Color online) Comparison of X-Y distributions for three focusing modes and GICOSY calculation results, for the reaction system  $^{32}\text{S} + ^{94}\text{Zr}$ . (a) X-Y distribution on focal plane for double-focusing mode at  $\theta_{\text{Lab}} = 55^\circ$  with ic pressure 60 torr (b) X-Y distribution on focal plane for Y parallel - X focusing mode at  $\theta_{\text{Lab}} = 50^\circ$  with ic pressure 50 torr (c) X-Y distribution on focal plane for X parallel - Y focusing mode for reaction system at  $\theta_{\text{Lab}} = 50^\circ$  with ic pressure 50 torr. For different focusing mode, the left panel is position spectra on the focal plane, given by IC. The right panel is GICOSY calculation results under the corresponding condition.

200 for more precise energy detection. Through the method described in section II, the images of X-Y distributions on the

202 focal plane for three focusing modes are shown in Fig. 9,  
 203 which were consistent with the distribution results calculated  
 204 by GICOSY. In this case, the magnetic field settings  $B_{Q2}/B_{Q1}$   
 205 of different focusing modes (a), (b) and (c) are 1.678, 1.32  
 206 and 1.577 respectively, with  $B_{Q1} = B_{Q3}$  at the same time. The  
 207 results of Fig. 9 verify the position resolution capability of IC  
 208 and the focusing performance of quadrupole triple lens.

209 The large effective solid angle and good charge and mass  
 210 resolution provide opportunities for measuring cross sections  
 211 of weak reaction channels. The  $\Delta E - E$  measurement, shown  
 212 in Fig. 10, identifies different elements precisely. The popu-  
 213 lated products isotopes at  $E_{\text{beam}} = 135$  MeV precisely extend  
 214 from  $Z = 12$  (4 proton stripping) to  $Z \leq 16$ . The lower energy  
 215 particle observed were elements C ( $Z = 6$ ) and O ( $Z = 8$ ) on  
 216 the targets and their backings.

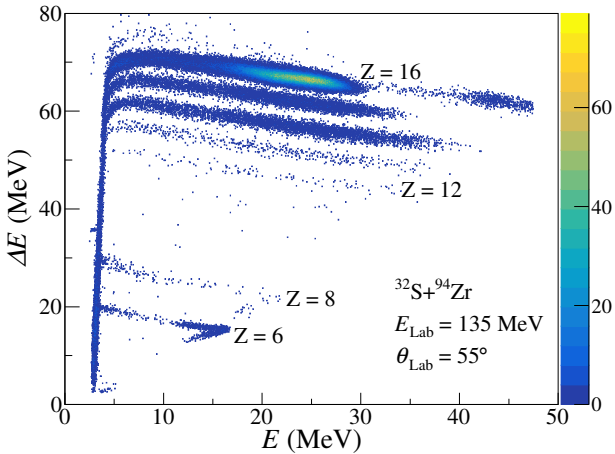


Fig. 10. (Color online)  $\Delta E - E$  matrix at  $\theta_{\text{Lab}} = 55^\circ$ . Different charges of projectile-like nuclears are clearly separated.

217 The resolution of HiToF spectrometer allows an unambigu-  
 218 ous identification of numerous projectile-like products. Mass-  
 219 charge two dimensional spectra were obtained for the reac-  
 220 tion  $^{32}\text{S} + ^{90,94}\text{Zr}$  at  $\theta_{\text{Lab}} = 55^\circ$  (close to the grazing angle),  
 221 as shown in Fig. 11. A number of reaction channels, includ-  
 222 ing proton stripping, neutron stripping and neutron pick-up  
 223 reaction are measured. Reaction products were clearly iden-  
 224 tified up to the pick-up of two neutrons and stripping of four  
 225 protons. Rare events belonging to the -5p channels were also  
 226 observed.

227 For the reaction system, IC provides a nuclear charge res-  
 228 olution  $\Delta Z/Z = \frac{1}{50}$ . The mass resolution achieved was  
 229  $\sigma = 0.2$  amu, which is mainly limited by the energy reso-  
 230 lution of IC.

231 Mass spectra for various  $Z$  selections are shown in Fig. 12  
 232 and Fig. 13. For  $Z = 16$ , an exponential decline of the ion  
 233 yield with an increasing number of transferred neutrons can  
 234 be observed. In Fig. 13, a number of channels from  $Z = 12$   
 235 to  $Z = 15$  are measured clearly. The peak with  $Z = 12$ ,  $A = 26$   
 236 corresponds to the -4p-2n channel.

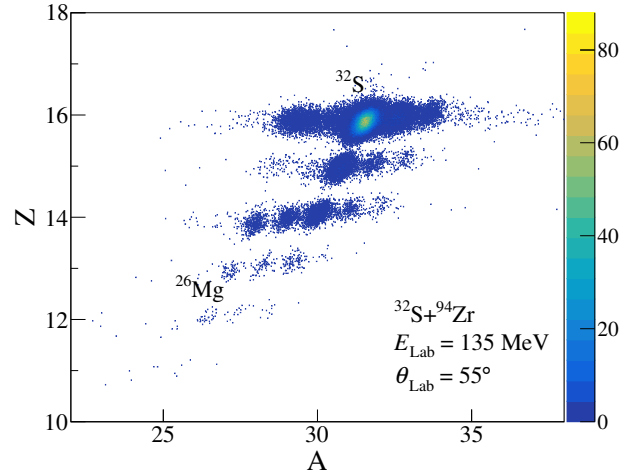


Fig. 11. (Color online) Z-A matrix at  $\theta_{\text{Lab}} = 55^\circ$ . The most intense spot at  $Z = 16$  corresponds to  $A = 32$ . The resolving power of HiToF facilitates the clear and definitive identification of a diverse array of projectile-like reaction products.

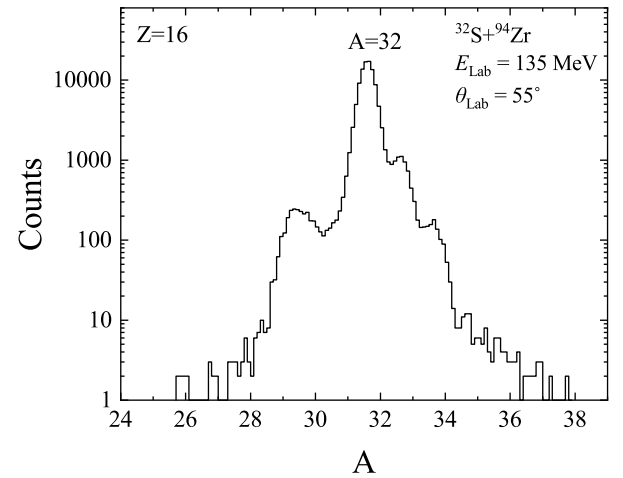


Fig. 12. Mass spectrum for S isotopes populated in the reaction  $^{32}\text{S}$  (beam) +  $^{94}\text{Zr}$  at  $\theta_{\text{Lab}} = 55^\circ$

#### IV. SUMMARY AND OUTLOOK

237 According to the test experiment, the HiToF spectrometer,  
 238 a simple and high-precision equipment which can provide a  
 239 large solid angle of 20 msr and allow a good resolution for  
 240 mass, energy and position, has been adequately prepared to  
 241 study multi-nucleon transfer reaction. The resolution of mass,  
 242 charge and position reach  $\sigma = 0.2$  amu,  $\Delta Z/Z = \frac{1}{50}$ , 1.0,  
 243 0.5 and 2.0 mm for X, Y and Z dimension, respectively. Dif-  
 244 ferent focusing modes of the quadrupole triplet lens provide  
 245 possibilities for various investigations. The energies and/or  
 246 masses can be investigated mainly limited by the resolving

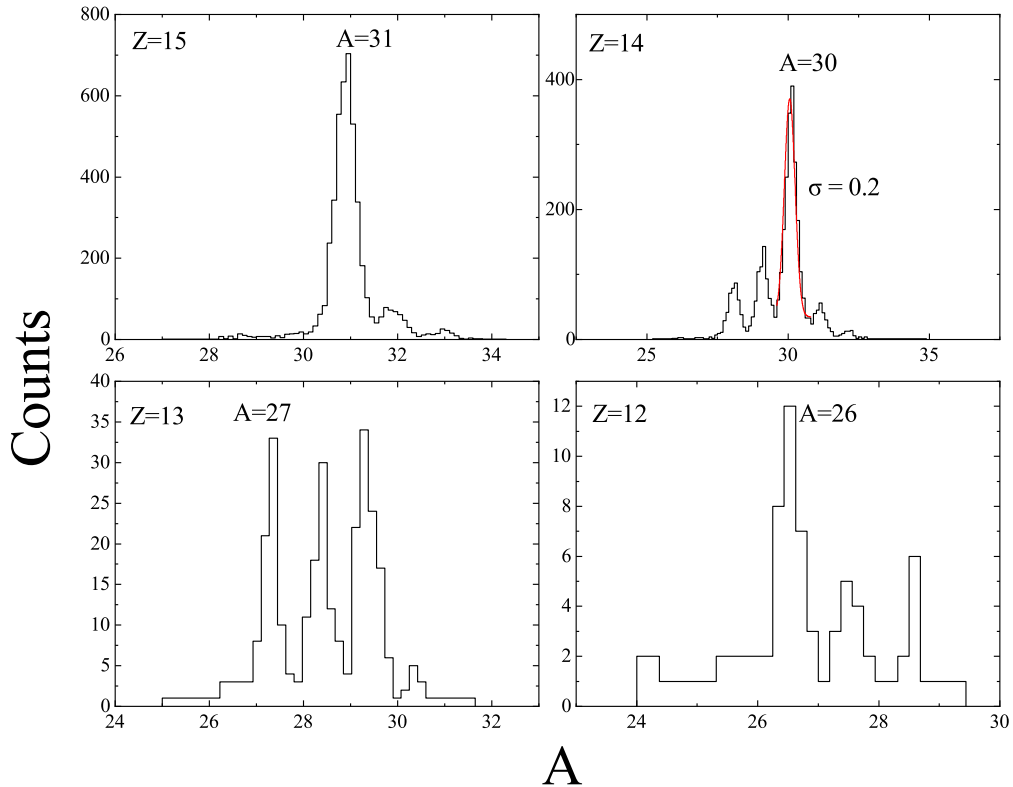


Fig. 13. (Color online) Projections on the mass matrix in  $^{32}\text{S}$  (beam) +  $^{94}\text{Zr}$  shown in Fig. 11, for different Z selections. The mass resolution is  $\sigma = 0.2$

power of the detection system, which fundamentally determines the performance of the spectrometer.

In the near future, the improved IC and the track reconstruction via the timing detector of ToF measurement and IC are would be combined to enhance the energy resolution with more precise magnetic field. An angle-distribution with higher precision would be given via the coincidence of IC for

measurement of projectile-like particles and  $v$ - $E$  detector for measurement of target-like particles.

For the field of low energy nuclear reaction, HiToF provides good opportunities for reaction mechanisms study experimentally. Superior performances of the device are required for frontiers, therefore some efforts will be made to improve the detection system such as enhancement of energy and position resolution.

---

[1] L. Corradi, A. M. Stefanini, C. J. Lin et al., Multinucleon transfer processes in  $^{64}\text{Ni} + ^{238}\text{U}$ . *Phys. Rev. C* **59**, 261 (1999). doi: [10.1103/PhysRevC.59.261](https://doi.org/10.1103/PhysRevC.59.261)

[2] T. Niwase, Y. X. Watanabe, Y. Hirayama et al., Discovery of New Isotope  $^{241}\text{U}$  and Systematic High-Precision Atomic Mass Measurements of Neutron-Rich Pa-Pu Nuclei Produced via Multinucleon Transfer Reactions. *Phys. Rev. Lett.* **130**, 132502 (2023). doi: [10.1103/PhysRevLett.130.132502](https://doi.org/10.1103/PhysRevLett.130.132502)

[3] R.R. Betts, Time of flight detectors for heavy ions. *Nucl. Instrum. Methods* **162**, 531 (1979). doi: [10.1016/0029-554X\(79\)90731-6](https://doi.org/10.1016/0029-554X(79)90731-6)

[4] L. Corradi, G. Montagnoli, D. R. Napoli et al., A kinematic coincidence technique for the study of low-energy heavy-ion reactions. *Nucl. Instrum. Methods A* **297**, 461 (1990). doi: [10.1016/0168-9002\(90\)91330-E](https://doi.org/10.1016/0168-9002(90)91330-E)

[5] G. Montagnoli et al., The time-of-flight spectrometer for heavy ions PISOLO. *Nucl. Instrum. Methods A* **454**, 306 (2000). doi: [10.1016/S0168-9002\(00\)00482-4](https://doi.org/10.1016/S0168-9002(00)00482-4)

[6] W. Starzecki, A.M. Stefanini, S. Lunardii et al., A compact time-zero detector for mass identification of heavy ions. *Nucl. Instrum. Methods* **193**, 499 (1982). doi: [10.1016/0029-554X\(82\)90242-7](https://doi.org/10.1016/0029-554X(82)90242-7)

[7] Wu, HK., Wang, XY., Wang, YM. et al. Fudan multi-purpose active target time projection chamber (fMeta-TPC) for pho-

287 tonuclear reaction experiments. NUCL SCI TECH 35, 200 297 [10] R. Bass, J.v. Czarnecki and R. Zitzmann, Design study  
288 (2024). doi: [10.1007/s41365-024-01576-1](https://doi.org/10.1007/s41365-024-01576-1) 298 of a magnetically focussed time-of-flight spectrometer for  
289 [8] Tian, J., Sun, ZP., Chang, SB. et al. Studies of an event-building 299 heavy ions. Nucl. Instrum. Methods **130**, 125 (1975). doi:  
290 algorithm of the readout system for the twin TPCs in HFRS. 300 [10.1016/0029-554X\(75\)90164-0](https://doi.org/10.1016/0029-554X(75)90164-0)  
291 NUCL SCI TECH 35, 73 (2024). doi: [10.1007/s41365-024-01434-0](https://doi.org/10.1007/s41365-024-01434-0)  
292 [9] Wang, DX., Lin, CJ., Yang, L. et al., Compact 16-channel 301 [11] M. Berz, H. C. Hoffmann, H. Wollnik, et al., COSY 5.0 -  
293 integrated charge-sensitive preamplifier module for silicon 302 The fifth order code for corpuscular optical systems. Nucl.  
294 strip detectors. NUCL SCI TECH 31, 48 (2020). doi: 303 Instrum. Methods A **258**, 402 (1987). doi: [10.1016/0168-9002\(87\)90920-X](https://doi.org/10.1016/0168-9002(87)90920-X)  
295 [10.1007/s41365-020-00755-0](https://doi.org/10.1007/s41365-020-00755-0) 304